Polymer(Korea), Vol. 40, No. 5, pp. 804-812 (2016)
http://dx.doi.org/10.7317/pk.2016.40.5.804

ISSN 0379-153X(Print)
ISSN 2234-8077(Online)

SiC 마이크로입자와 그래핀 옥사이드가 그래프트된 SiC 나노입자를 포함하는 감압점착제의 열전도도 향상

부민칸 · 박규대 · 배영한 · 김성룡†

한국교통대학교 나노화학소재공학과

(2016년 5월 12일 접수, 2016년 6월 10일 수정, 2016년 6월 10일 채택)

Enhanced Thermal Conductivity of Pressure Sensitive Adhesives Using Hybrid Fillers of SiC Microparticle and SiC Nanoparticle Grafted Graphene Oxide

Minh Canh Vu, Gyu-Dae Park, Young-Han Bae, and Sung-Ryong Kim†

Department of Polymer Science and Engineering, Korea National University of Transportation, Chungju 27469, Korea

(Received May 12, 2016; Revised June 10, 2016; Accepted June 10, 2016)

초록: SiC 마이크로입자를 주필러로 사용하고 그래핀 옥사이드가 그래프트된 SiC 나노필러를 보조필러로 사용한 UV 경화형 감압점착제의 열전도도에 대하여 연구하였다. 개질된 SiC 나노필러와 그래핀 옥사이드를 결합시킨 필러($mSiC_{nano}$-GO)를 도입한 결과 필러의 침전이 발생하지 않는 균일한 분산을 얻었다. 전체 필러의 함량을 고정시킨 상태에서 SiC 마이크로입자를 $mSiC_{nano}$-GO로 0.5-2.0 wt% 대체하여 감압점착제의 열전도도와 점착력의 현저한 증가를 관찰하였으나, $mSiC_{nano}$-GO의 함량이 증가함에 따라 감압점착제의 박리강도는 감소하였다. 40 wt%의 하이브리드 필러를 포함하는 감압점착제의 열전도도는 0.68 W/m·K로 순수 점착제에 비하여 325% 증가하였다. 이와 같은 증가는 보조필러와 기재와의 화학결합과 SiC 마이크로필러와 mSiC-GO 사이에 형성된 열전달 경로 때문으로 여겨진다.

Abstract: Thermal conductivity of UV-crosslinked pressure sensitive adhesives (PSAs) using SiC microparticle as a main filler and SiC nanoparticle grafted graphene oxide ($mSiC_{nano}$-GO) as an auxiliary filler have been investigated. The introduction of $mSiC_{nano}$-GO resulted in a homogeneous distribution of fillers without the sedimentation of SiC microparticle. The thermal conductivity and initial tack of PSAs was significantly increased with substituting 0.5-2.0 wt% of $mSiC_{nano}$-GO filler for SiC microparticle at a fixed total weight fraction of fillers in PSAs, however, the peel strength of PSAs decreased with increasing the $mSiC_{nano}$-GO fillers. The PSAs showed the thermal conductivity of 0.68 W/m·K at 40 wt% of hybrid filler content which is a 325% improvement compared to the bare-PSA. It is speculated that the enhancement is due to the auxiliary filler chemically bonded with matrix and the facile formation of heat paths between SiC_{micro} and $mSiC_{nano}$-GO.

Keywords: pressure sensitive adhesives, hybrid fillers, thermal conductivity, graphene oxide, grafting.

Introduction

Pressure sensitive adhesives (PSAs) are viscoelastic-elastomeric materials and stick on surfaces when pressure is applied. Since their introduction half a century ago, PSAs are generally used in many applications such as package, electronic devices, medical products, and automobiles.[1] PSAs require the balanced properties of tackiness, peel strength and shear strength for each specific application.

PSAs can be produced via different polymerization processes such as hot-melt, solution polymerization and emulsion polymerization and they have excellent properties such as transparency, colorlessness and resistance to yellowing from sunlight or oxidation.[2,3] However, the linear acrylic chains in PSAs are not generally cross-linked with chemical bonds but connected physically due to van der Waals forces or hydrogen bonding interactions with the carboxylic group resulting in the relatively poor mechanical and thermal properties.[4]

One of methods to improve the thermal and mechanical properties of acrylic chains is to crosslink the acrylic chains in

†To whom correspondence should be addressed.
E-mail: srkim@ut.ac.kr

PSAs by conventional thermal curing or UV-curing. UV-based PSAs can be made by UV-polymerization and UV-crosslinking. UV-polymerized PSAs are made by blending oligomers, monomers, photo-initiators and then exposed to UV-irradiation. The UV-crosslinking method has various advantages including fast reaction rates, low power consumption, low volatile organic contents, high chemical stability, lower environmental pollution as well as improved applicability to high temperature substrates.[5]

Due to the slim design and increased power consumption, the heat dissipation power density increases rapidly in the electronic devices. It is known that the performance, reliability and further miniaturization of electronic devices is strongly dependent on the operation temperature and the effective heat dissipation is very important for the electronic devices.[6-8] The reliability of an electronic device is dependent exponentially on the operating temperature of the device, whereby a small difference in operating temperature can extend the service life of that electronic device. Therefore, it is essential to dissipate the generated heat from the devices as quickly as possible to maintain the desired operating temperature.[6,9,10] In addition, the design of the electric devices requires a thermally conductive pressure sensitive adhesives to form a bond and provide an effective heat pathway between heat-generating parts and heat sinks. Pressure sensitive adhesives loaded with thermally conductive fillers is one of the best candidate for these purposes. Accordingly, the increased use of thermally conductive PSAs is emerging as cost-effective ways of addressing thermal management issues.

The commercially available polymeric materials, including adhesives, have thermal conductivities near 0.20 W/(m·K), which is far below that of metal or ceramic fillers. It is well known that polymers filled with thermal conductive fillers show a distinctive dependence of thermal conductivity on the filler content.

Graphene oxide (GO) has attracted interest in the last years for a wide range of applications including electronic devices,[11] optical applications,[12] catalysis[13] and super capacitors[14] owing to their superior properties such as large surface area, high intrinsic mobility, high optical transmittance and high thermal conductivity.[15] Graphene oxide contains abundant functional groups such as epoxide, hydroxyl and carbonyl groups; These can be well dispersed and exfoliated in the polymer matrix at low filler content due to its good interaction with polymer chains.[16,17] However, because of the high surface area, van der Waals interaction, and vacuum filtration in the preparation process, GO has a tendency to form severe aggregations at a high loading and its prominent properties decrease in the polymer.[18,19]

Recently, numerous processing methods like *in-situ* polymerization, decoration and grafting nanoparticles on the surface and organic modification have been proposed to improve dispersion and exfoliation of graphene oxide. Nanoparticles grafting on graphene oxide provided efficient separation of graphene oxide sheets and many nanoparticles, such as Al_2O_3,[20] SiO_2,[21] MgO,[22] were utilized for grafting. Many studies used nanoparticles to graft on graphene oxide applied for super-capacitors[23] and catalysts,[24] electrodes,[25] but there are no reports showing the effect on thermal conductivity of PSAs when nanoparticles are grafted on the graphene oxide surface.

In this study, we have prepared the thermally conductive acrylic based pressure sensitive adhesives using UV-crosslinking. Silicon carbide microparticles (SiC_{micro}) of high thermal conductivity (~390 W/m·K) were used as a main filler.[26] In addition, we also have developed a route to prepare covalently bonded silicon carbide nanoparticle ($mSiC_{nano}$)-GO fillers, which have important properties as an auxiliary filler in the PSAs matrix. The $mSiC_{nano}$-GO nanocomposites were synthesized with the help of 3-aminopropyl trimethoxysilane (APTMS) in which the amine group of APTMS conjugated to the oxygen functional groups on the graphene oxide surface. Finally, the properties of the UV-crosslinked PSAs according to the amount of fillers and their effects on the morphology, adhesion strength, initial tack and thermal conductivity of PSAs were investigated.

Experimental

Materials. 2-Ethylhexyl acrylate (2-EHA), acrylic acid (AA), methyl methacrylate (MMA), and glycidyl methacrylate (GMA) were purchased from Sigma Aldrich Co., USA and used as received without purification. 1-Benzoyl-1-hydroxycyclohexane (Irgacure 184, Ciba Co., Switzerland) and 2,4,6-trimethylbenzoyl-diphenyl-phosphine oxide (Darcure TPO, Sigma Aldrich Co., USA), were used as photoinitiators and the multifunctional monomer trimethylolpropane triacrylate (TMPTA, Sigma Aldrich Co., USA) was used as crosslinking agent. Polyethylene terephthalate (PET) substrate (SKC Co., South Korea) with a thickness of 73 μm and size of 100 mm×150 mm was used as a release film. Graphene oxide (GO, Graphene Supermarket Co., USA), SiC nanoparticles (β-SiC, particle size of 100 nm, CNvision Co., South Korea), SiC micropar-

ticles (β-SiC, particle size of 70 μm, Sigma Aldrich Co., USA) were used as fillers. Thionyl chloride ($SOCl_2$), hydrofluoric acid (HF), (3-aminopropyl) trimethoxysilane (APTMS), anhydrous tetrahydrofuran (THF) and N,N-dimethylformamide (DMF) were purchased from Sigma Aldrich Co. and used as solvents to modify fillers.

Pre-polymer Synthesis. The pre-polymer was prepared by UV-polymerization without the use of solvent. 70 wt % of 2-EHA, 12 wt% of GMA, 10 wt% of AA, 8 wt% of MMA and 0.02 wt% of photo-initiator (Irgacure 184) were placed into a 500 mL four-neck round bottom flask with a mechanical stirrer and thermometer. The wavelength of the UV lamp was 365 nm. The distance from the UV lamp (10 W) to the flask was 20 cm. After the UV-polymerization, 0.5 wt% of TMPTA, 2 wt% of Irgacure 184 and 2 wt% of Darcure TPO were added and stirred for 20 min to prepare the pre-polymer.

Preparation of Surface Modification of SiC Nanoparticles Using APTMS. Silicon carbide (0.1 g) nanoparticles (SiC_{nano}) were dispersed into 30 mL of aqueous HF – ethanol mixture (10/90, v/v) and sonicated for 30 min at room temperature to activate the SiC_{nano} surface by introducing hydroxyl groups for silanization. After the HF treatment, the SiC_{nano} were filtered and dried at 70 °C for several hours. Subsequently, the samples were added to a three-neck round flask containing 50 mL toluene and dispersed by sonication for 30 min. Then, 0.1 mL APTMS was added drop-wise to the above solution and the mixture was then stirred for 6 h at 60 °C to allow silanization. After the reaction, 30 mL of ethanol was added to dilute unreacted APTMS molecules. The product was prepared by filtration and washing with ethanol and DI water. The silane modified SiC_{nano} particles ($mSiC_{nano}$) were dried in a vacuum oven at 70 °C for 12 h.

Preparation of Acyl Chlorides of Graphene Oxide (GOCl). Graphene oxide (0.3 g) was added to a 500 mL round bottom flask containing 50 mL thionyl chloride ($SOCl_2$) and 2.5 mL N,N-dimethylformamide (DMF), and sonicated at room temperature for 1 h to form a suspension. The mixture was stirred at 70 °C for 24 h. Then, the excess $SOCl_2$ was evaporated by distillation. After washing with anhydrous tetrahydrofuran (THF) and drying at 70 °C in a vacuum, a dark powder (GOCl) was obtained.[27,28]

Grafting of $mSiC_{nano}$ Particles on Graphene Oxide ($mSiC_{nano}$-GO). GOCl (0.3 g) was dispersed on 50 mL anhydrous tetrahydrofuran (THF) and sonicated for 1 h at room temperature. Then, 0.1 g of $mSiC_{nano}$ particles were added to the mixture with the mass ratio of 1:3.[29] After being sonicated

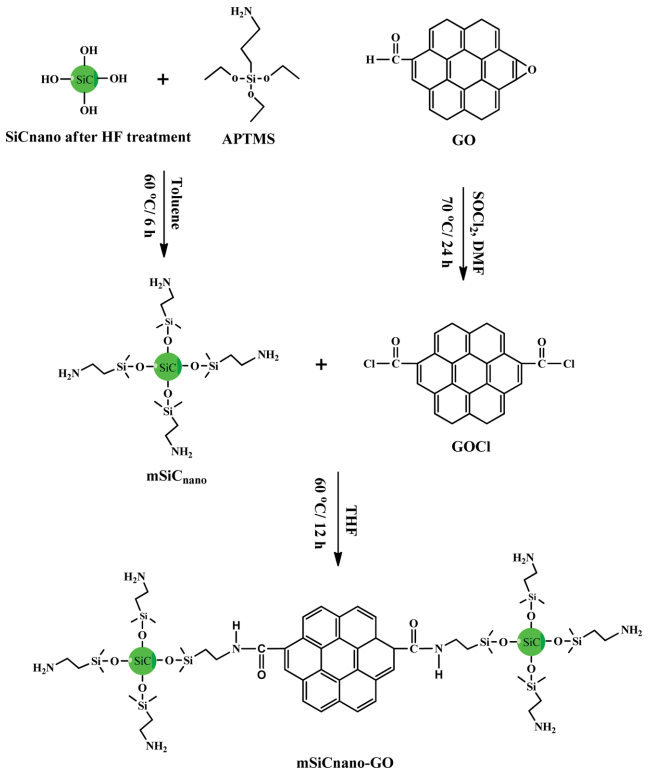

Figure 1. Schematic steps to graft modified SiC nanoparticles on GO ($mSiC_{nano}$-GO).

for another 1 h, the mixture was stirred for 12 h at 60 °C. A dark solid was obtained by filtering and washing with the mixture in ethanol and DI water (1:1). The final product ($mSiC_{nano}$-GO) in Figure 1 was obtained after drying for 12 h at 70 °C in a vacuum.

Preparation of PSAs. The $mSiC_{nano}$-GO and SiC_{micro} particles were mixed as fillers in UV-polymerized pre-polymer PSA for 10 min at 1000 rpm using a paste mixer (HPM-500, Hantech Co., South Korea). In an attempt to prevent the aggregation of SiC_{micro} fillers and obtain high thermal conductivity, we have replaced some of the main SiC_{micro} particles by $mSiC_{nano}$-GO fillers. The mixture of fillers and PSA was poured onto a release PET film and was made into film using a custom-built mold. The film was stored at room temperature for 1 h and then UV-cured using a UV chamber equipped with a mercury lamp (wavelength 365 nm, power intensity 3 mJ/cm^2/s, 600 W), and the UV dose was 2000 mW/cm^2. The dried films were kept at 23±2 °C and 60±5% RH for 24 h before testing.

Characterization of Samples. Fourier transform infrared (FTIR, Nicolet IR 200, Thermo Electron Co., USA) spectra were analyzed in respect to the surface composition of modified SiC_{nano}, acyl chlorides of graphene oxide and $mSiC_{nano}$-

GO. The size, shape and dispersion of the fillers in the PSA matrix were examined using a field emission scanning electron microscope (FESEM, JEOL Co., 6700F, Japan). Energy-dispersive X-ray spectroscopy (EDX) was used to demonstrate the grafting of $mSiC_{nano}$ particles on the GO surface.

Thermal conductivity of each sample was measured at room temperature by thermal conductivity analyzer (Quickline-10®, Anter Co., USA). A sample with diameter of 50 mm and thickness of 1 mm was used.

The sample for peel strength was prepared by coating PSAs onto a PET film with a thickness of 0.25 mm, and then pressed onto stainless steel substrate twice by a roller 2 kg. The peel strength was measured based on ASTM D3330 by using an analyzer (SurTA 1A, Chemilab Co., Korea) with the speed of 5 mm/s at room temperature. Initial tack of each sample which had a thickness of 1 mm was measured according to ASTM D2979 by using the same texture analyzer with crosshead speed of 0.05 mm/s, contact time of 2 s, and loading force of 200 g_f. The thermal degradation of each sample was measured using a thermal gravimetric analyzer (TGA, TA 1000, TA Instrument Co., USA) from room temperature to 700 °C with a heating rate of 10 °C/min in a nitrogen atmosphere.

Results and Discussion

Characterization of $mSiC_{nano}$-GO. Fourier transfer infrared was utilized to investigate the modification and grafting process. The transmission FTIR spectra of SiC_{nano}, SiC_{nano} after HF treatment, modified $mSiC_{nano}$, GO, GOCl and $mSiC_{nano}$-GO are shown in Figure 2. In the spectrum of unmodified SiC nanoparticles (SiC_{nano}), the peak at 860 cm^{-1} can be assigned to the stretching vibration of Si-C bonds. In the spectrum of SiC_{nano} particles after treating with the mixture of ethanol and HF shows broad peaks at 3400 and 1630 cm^{-1}, which are attributed to the O-H stretching vibrations.[30] The absorption peaks at 860 and 730 cm^{-1} are related to the Si-C and Si-O stretching vibrations, respectively. After surface modification of SiC_{nano} by APTMS, the peak at 3400 cm^{-1} became weaker and the peaks at 2850 and 2925 cm^{-1} appeared, representing the asymmetric and symmetric stretching of $-CH_2$ groups from alkyl chains connecting with the NH_2 group. The peak of Si-O-Si bonding at around 1030 and 1125 cm^{-1} implies the successful interaction between -OH groups on SiC_{nano} particles and $-OCH_3$ groups of APTMS molecules.[31,32] The broadening of absorption band in the region near 1560 cm^{-1} can be assigned to the N-H bending of primary amines ($-NH_2$). The spectrum of $mSiC_{nano}$ confirms that APTMS is attached onto the SiC nanoparticle surface.

As presented in Figure 2(b), the characteristic absorption peaks of GO at 3400 cm^{-1} (-OH), 1730 cm^{-1} (C=O) 1625 cm^{-1} (C=C), 1222 cm^{-1} (C-O-C) and 1045 cm^{-1} (C-O), confirm that the GO surface is attached with the hydroxyl, carboxyl, car-

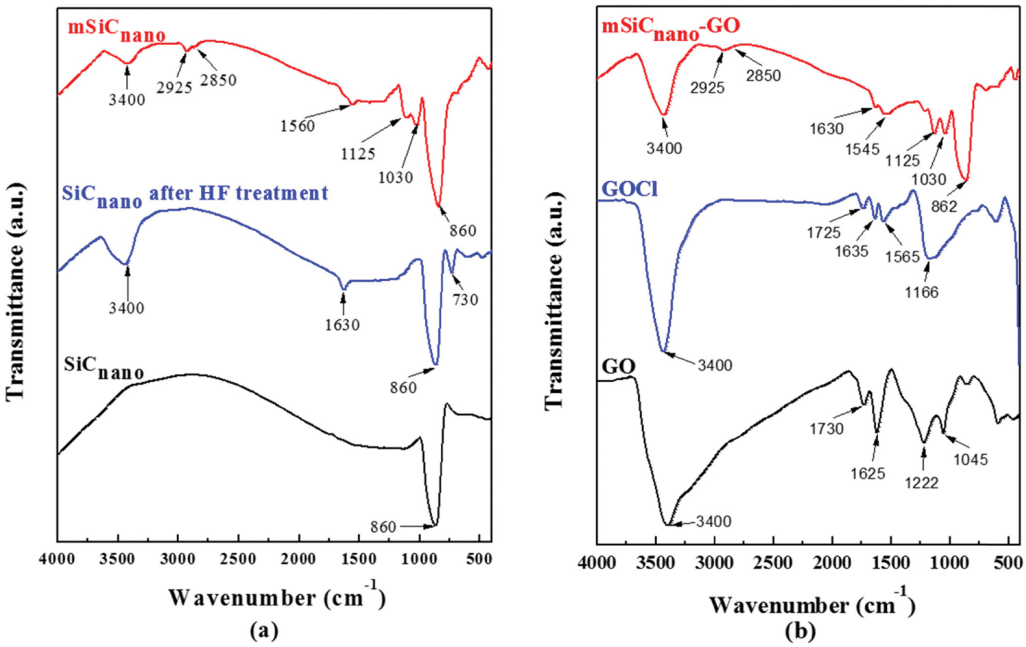

Figure 2. FTIR spectra of (a) SiC_{nano}, SiC_{nano} after HF treatment, $mSiC_{nano}$; (b) GO, GOCl, and $mSiC_{nano}$-GO.

boxylic and epoxy groups.[33] The FTIR spectrum of GOCl indicates that the oxygen group is retained on the GO surface. As can be seen, the appearance of a broad peak around 1166 cm^{-1} and the C=O stretching peaks are shifted to 1725, 1635, 1565 cm^{-1} indicating the formation of the COCl group.[34] In the FTIR spectrum of $mSiC_{nano}$-GO, the characteristic absorption peaks of GO and $mSiC_{nano}$ were shown. The disappearance of the peak at 1166 cm^{-1} and new peak at 1545 cm^{-1} indicate the secondary amide N-H- bending and C-N stretching,[35] and imply the reaction between the acyl chloride groups on the GO surface and amine groups on the $mSiC_{nano}$. All of these results above demonstrate the successful grafting of $mSiC_{nano}$ onto the GO surface through chemical bonding.

Morphology. Field emission scanning electron microscope (FE-SEM) micrographs in Figure 3 show the characteristic morphology of SiC particles and PSAs with fillers. Figure 3(a), (b) shows that the smooth surface of SiC_{micro} particles have an average size of 70 μm with a range of 30-100 μm and $mSiC_{nano}$ particles have an average size of 100 nm ranging from 70-150 nm. As presented in Figure 3(c), after grafting by $mSiC_{nano}$, the GO sheets exhibited a well exfoliated GO with a rough surface. Also, the $mSiC_{nano}$ particles were attached at various points on the GO surface.

Figure 4 shows the morphology of PSA composites loading at total 30 wt% of fillers. Due to high gravity and subsequent sedimentation of SiC_{micro} fillers (white circle) during the curing step, the composites show aggregated fillers in the PSA matrix (Figure 4(a)). The poor wettability of SiC_{micro} particles revealed voids (white arrows) on the fractured surfaces at the higher magnification of SiC_{micro}/PSA composites (Figure 4(e)). Figure 4(b), (f) shows the fractured surface of 2 wt% of SiC_{nano}/28 wt% of SiC_{micro} filled PSA composites. There was no sedimentation, but the composites still show the aggregated SiC_{micro} particles and voids. The PSA composites of 2 wt% of GO and 28 wt%

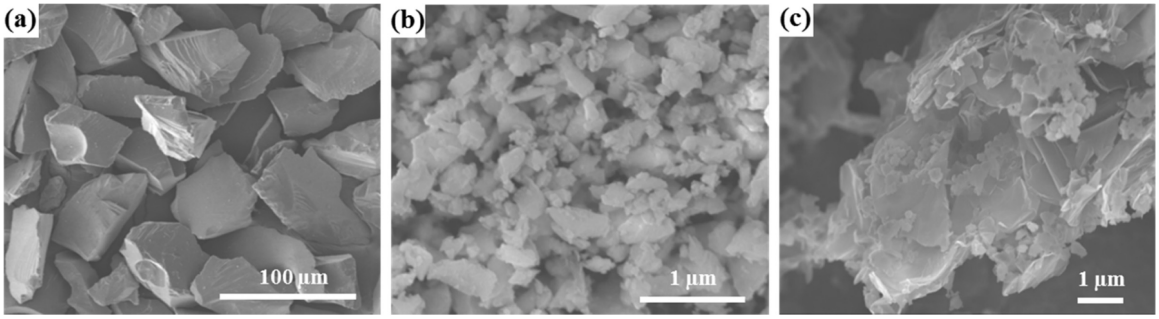

Figure 3. FE-SEM micrographs of (a) SiC_{micro} particles; (b) SiC_{nano} particles; (c) $mSiC_{nano}$-GO.

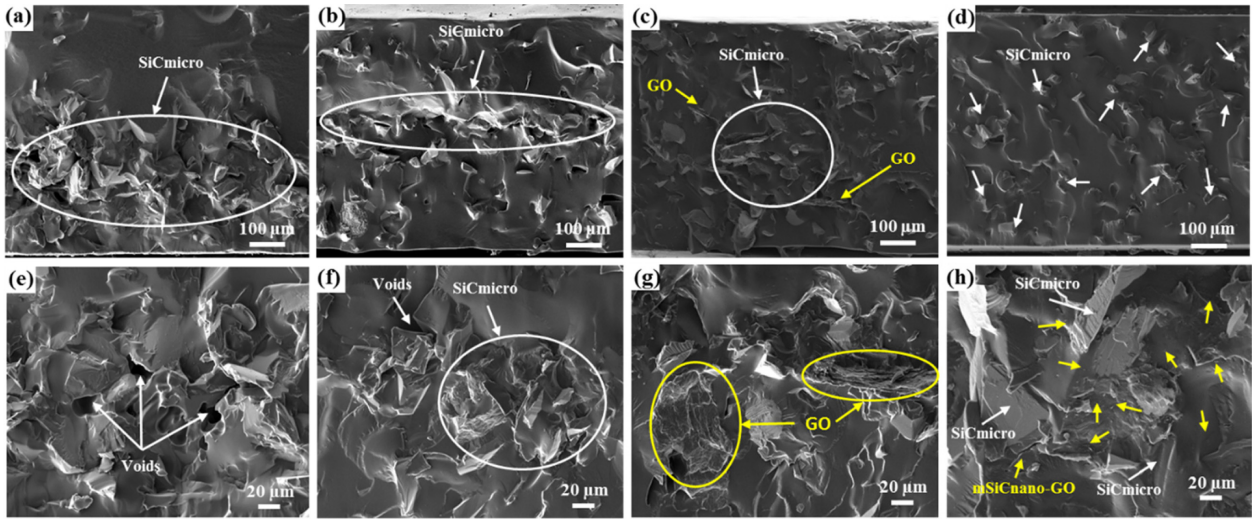

Figure 4. FE-SEM micrographs of (a) 30 wt% SiC_{micro} filled PSA composites; (b) 2 wt% SiC_{nano}/28 wt% SiC_{micro} filled PSA composites; (c) 2 wt% GO/28 wt% SiC_{micro} filled PSA composites; (d) 2 wt% $mSiC_{nano}$-GO/28 wt% SiC_{micro} filled PSA composites; (e, f, g, h) is the higher magnification of (a, b, c, d), respectively.

of SiC_{micro} also resulted in the agglomeration of SiC_{micro} particles (white circle) in Figure 4(c) and GO (yellow arrows and circles) in Figure 4(g). The high surface area and van der Waals interaction of GO may cause a severe aggregation. The poor dispersion of fillers could cause a phonon scattering and short mean free path and possibly reveal a low thermal conductivity of the composites. The hybrid fillers of 2 wt% $mSiC_{nano}$-GO and 28 wt% of SiC_{micro} in the PSA matrix revealed uniformly dispersed fillers without any aggregation or sedimentation as shown in Figure 4(d), (h). It is speculated that the chemical bonding between SiC_{nano} and GO effectively prevent the agglomeration of GO and the covalent bonding between $mSiC_{nano}$-GO and the matrix may responsible for the uniform dispersion.

Thermal Conductivity. Figure 5(a) shows the thermal conductivities of bare PSA and PSAs with several weight percentages of SiC_{micro} and $mSiC_{nano}$-GO fillers. The thermal conductivity of UV-crosslinked PSA without fillers was 0.16 W/(m·K). The thermal conductivity of PSAs increased with increasing filler content. The thermal conductivity of PSA with SiC_{micro} fillers only increased slightly even at higher weight fraction of filler. The thermal conductivity of PSAs was 0.22 W/(m·K) at 20 wt% of SiC_{micro} but it gradually increased by increasing the filler content and the thermal conductivity reached 0.32 W/(m·K) at 40 wt% of SiC_{micro}. The small increase of thermal conductivity could be due to the large size of SiC_{micro} fillers along with an aspect ratio of near unity, which is relatively difficult to form thermal paths. Also, the trapped voids between filler and matrix could have caused little increase in thermal conductivity.

As we can see in Figure 5(a), by replacing the part of SiC_{micro} fillers with up to 2 wt% of $mSiC_{nano}$-GO fillers, the thermal conductivity of PSAs significantly increased. The thermal conductivity of PSA was enhanced more than 2 times by introducing 2 wt % of $mSiC_{nano}$-GO fillers at the same total weight fraction of fillers. The thermal conductivity at 40 wt % of total fillers was 0.68 W/(m·K) which indicates more than 325% improvement in comparison with the bare-PSA. It is speculated that the thermal conductivity of composites is improved by using highly conducting nanoparticles on graphene oxide. Also, the GO grafted by $mSiC_{nano}$ with silane group becomes a structural component of the cross-linked PSA matrix by the formation of covalent bonding and it would reduce the interfacial phonon scattering and the interfacial thermal resistance and subsequently increase the thermal conductivity. In addition, $mSiC_{nano}$-GO could be filled between SiC microparticles to form a conducting path as shown in Figure 5(b). Consequently, there is enhanced inter-connectivity between SiC_{micro} and $mSiC_{nano}$-GO without any sedimentation of SiC_{micro} fillers and subsequent high thermal conductivity of PSAs with low filler content.

Figure 6 compares the effect of hybrid fillers on thermal conductivity of PSA composites at total 30 wt% (Figure 6(a)) and 40 wt% (Figure 6(b)) of fillers loading in which 2 wt% of SiC_{micro} particles replaced by 2 wt% of SiC_{nano}, GO and $mSiC_{nano}$-GO. It is evident that the increase of the thermal conductivity of PSA composites containing the hybrid fillers of SiC_{nano} and GO with SiC_{micro} particles in PSA matrix was marginal, however, that of PSA composites containing the hybrid

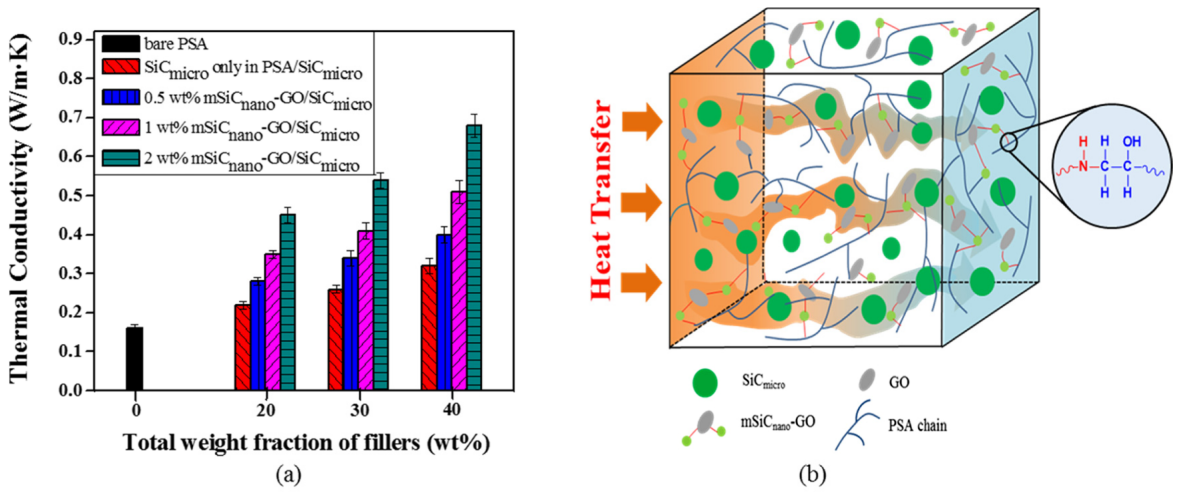

Figure 5. (a) Thermal conductivity of PSA composites as a function of filler content; (b) Scheme heat conducting path in the PSA composites with fillers.

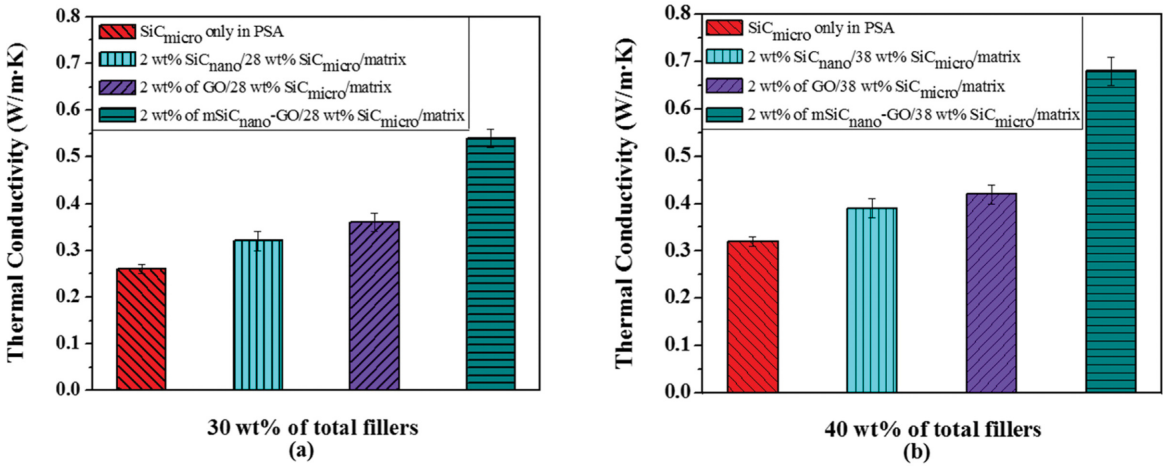

Figure 6. Thermal conductivity of PSA composites with total weight content of fillers at (a) 30 wt%; (b) 40 wt%.

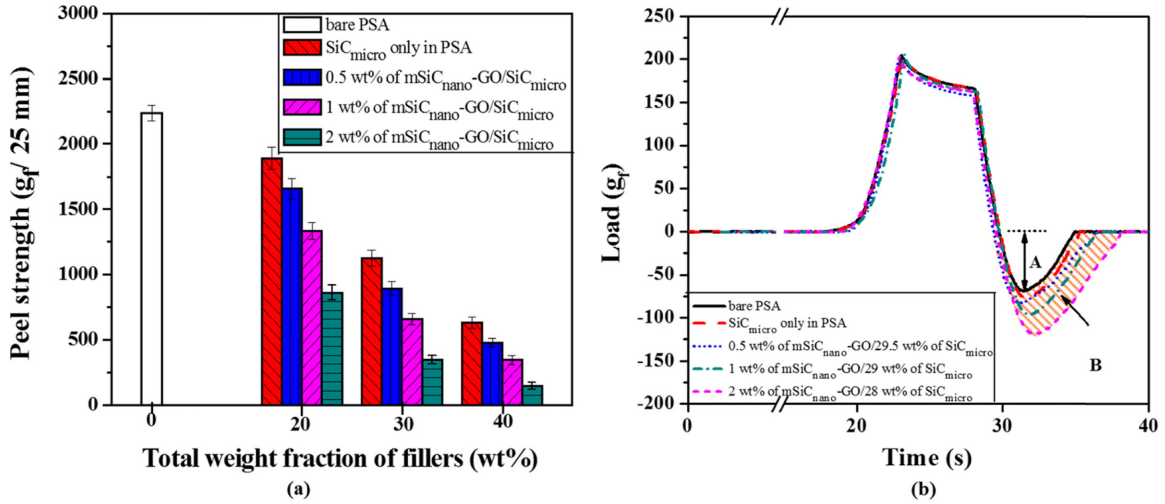

Figure 7. (a) Peel strength of PSA composites as weight fraction of fillers in PSAs matrix; (b) Initial tack of total weight fraction 30 wt% of SiC_{micro} and $mSiC_{nano}$-GO fillers in PSAs.

fillers of $mSiC_{nano}$-GO and SiC_{micro} was significant compared to the thermal conductivity of PSA composites with SiC_{micro} particles only. At total weight fraction of 30 wt% fillers in PSA matrix, thermal conductivities of 2 wt% of SiC_{nano} and 28 wt% of SiC_{micro} filled PSA composites, 2 wt% of GO and 28 wt% of SiC_{micro} filled PSA composites, and 2 wt% of $mSiC_{nano}$-GO and 28 wt% of SiC_{micro} filled PSA composites were 0.32 W/(m·K), 0.36 W/(m·K) and 0.54 W/(m·K), respectively, corresponding the enhancement of 23, 39 and 108%, respectively, compared with the PSA composites containing SiC_{micro} particles only. At total weight fraction of 40 wt% fillers in the PSA matrix, the thermal conductivity of PSA composites replaced by 2 wt% of $mSiC_{nano}$-GO filler was higher than those replaced by the same amount of SiC_{nano} and GO by 75% and 62%, respectively. There was no sedimentation when mixing the SiC_{micro} with SiC_{nano} or GO, however, the SiC_{micro} particles were still agglomerated in the PSA matrix. It could improve the thermal conductivity of the PSA composites with the hybrid fillers of SiC_{micro} particles with SiC_{nano} and GO.

Peel Strength and Initial Tack. The peel strength between PSA and steel substrate as a function of total weight fraction of fillers was shown in Figure 7. It is noticeable that peel strength of PSA composites decreased when increasing the weight fraction of fillers.

It is clearly seen that there was a downward trend of the peel strength when increasing the amount of auxiliary $mSiC_{nano}$-GO fillers replacing SiC_{micro} fillers at the same total weight fraction of fillers in PSAs. At 20 wt% of total fillers in PSAs, the peel

strength decreased from 1680 g_f/(25 mm) to 820 g_f/(25 mm) with increased amount of auxiliary filler by replacing the main filler from 0.5 to 2 wt%. A decline in the peel strength when we increase the content of $mSiC_{nano}$-GO at a fixed total weight fraction of fillers may attributed to the higher surface area of $mSiC_{nano}$-GO fillers, the increase of the uncured region represented by the shaded area (B) in Figure 7(b), and the subsequent decrease of internal cohesive strength of the matrix. Park *et al*. also reported the sharp decrease of the peel strength when GO was dispersed in the PSAs using *in-situ* polymerization method and the minimized reduction of peel strength by applying a bare PSA layer onto the GO dispersed PSA layer.[36]

We observed the decrease of the initial tack with increasing total amount of fillers (not shown). It is known that the initial tack is related to the wetting of the particles in the matrix. The higher amount of total fillers may induce the poor wetting and decrease the initial tack. The similar results were published by Czech *et al*. and Kim *et al*..[37,38] However, the initial tack of PSAs at the same total amount of fillers increased with increasing the content of auxiliary fillers. As can be seen in Figure 7(b), the initial tack of PSA composites at total weight fraction of 30 wt% of fillers increased with the higher percentage of $mSiC_{nano}$-GO loading.

The replacing SiC_{micro} fillers with $mSiC_{nano}$-GO of auxiliary fillers could improve the wetting of fillers and provide larger contact area of the probe, and increase the initial tack of PSAs. Also, the insufficient UV-crosslinking by the additional blocking of UV irradiation at higher amount of $mSiC_{nano}$-GO loadings, implied by the shaded area (B) in Figure 7(b) may increase the initial tack of the PSAs.

Thermal Stability. Figure 8 shows the effect of fillers on the thermal stability of PSAs with different filler loadings. Thermal decomposition of PSAs starts near 150 °C and the main weight loss takes place around 350-450 °C which is attributed to the degradation of the PSA matrix. The residue of the bare-PSA is less than 5 wt% at 600 °C. The PSA filled with 30 wt% of fillers starts to decompose at a higher temperature than bare-PSA and the decomposition temperature at 5 wt% of weight loss increased by 14-30 °C compared with the unfilled PSA. The temperature at 50 wt% weight loss of bare-PSA was about 405.2 °C, while the corresponding values of PSAs composites with auxiliary filler contents increasing from 0.5 to 2 wt% elevated by 18.1 to 23.7 °C, respectively. This indicates that the thermal stability of PSA obviously enhanced with a little amount of auxiliary filler. It can be explained by the uniformly dispersed auxiliary fillers with a higher surface area in the PSA matrix and the strong chemical bonding between $mSiC_{nano}$-GO auxiliary filler with PSA matrix helps it becomes more thermally stable than bare-PSA.

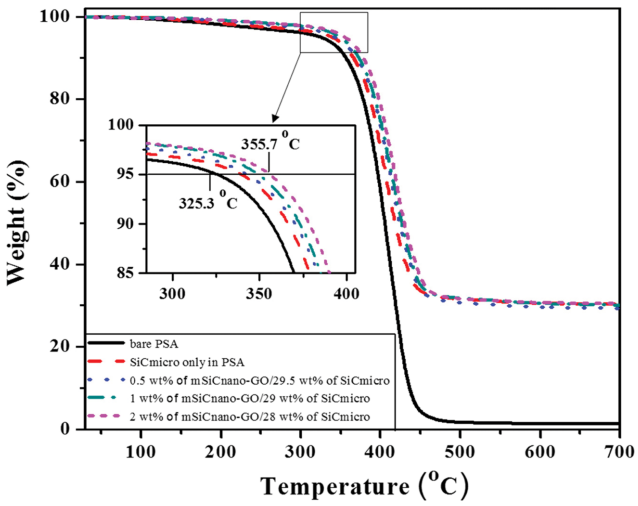

Figure 8. Thermal stability of PSA with 30 wt% of total fillers.

Conclusions

SiC_{micro} and $mSiC_{nano}$-GO as main and auxiliary fillers, respectively, were used to prepare thermally conductive PSAs. The APTMS modified SiC_{nano} particles were grafted on the GO surface by chemical bonding between amino groups and acyl chlorides. By replacing the part of SiC_{micro} fillers with up to 2 wt% of $mSiC_{nano}$-GO fillers resulted in uniform dispersion of fillers in the matrix without any sedimentation of SiC_{micro} and significant improvement of thermal conductivity and thermal stability. The thermal conductivity of PSAs increased by 325% with 38 wt% of SiC_{micro} and 2 wt% of $mSiC_{nano}$-GO loading over a bare-PSA. The chemical bonding and easy phonon transfer between GO and the acrylic matrix resulted in the improved thermal conductivity of PSAs.

The peel strength of PSAs showed a gradual decrease by replacing the main SiC_{micro} filler with small amount of $mSiC_{nano}$-GO filler. It was related to the decreased internal cohesive strength due to insufficient UV-crosslink. However, the initial tack of PSAs gradually increased when increasing the content of $mSiC_{nano}$-GO filler. The higher initial tack of auxiliary filler filled PSAs could be attributed to the smoother surface and the larger contact area of the probe. This study provides an insight how to improve the thermal conductivity and to retain the peel strength of the UV-crosslinked PSAs by introducing covalent bonded $mSiC_{nano}$-GO auxiliary filler with the matrix.

Acknowledgment: This research was financially supported by the Ministry of Education (MOE) and National Research Foundation of Korea (NRF) through the Human Resource Training Project for Regional Innovation (No. 2013H1B8A2032161). Also, this research was supported by The Leading Human Resource Training Program of Regional Neo industry through the National Research Foundation of Korea (NRF) funded by the Ministry of Science, ICT and future Planning (2016H1D 5A1908330).

References

1. S. Sun, M. Li, and A. Liu, *Int. J. Adhes. Adhes.*, **41**, 98 (2013).
2. C. Fang, B. Huang, and Z. Lin, *J. Appl. Polym. Sci.*, **131**, 40095 (2014).
3. D. Satas, *Handbook of Pressure-Sensitive Adhesive Technology*, 3rd ed., New York, Reinhold, 1999.
4. H. Do, J. Park, and H. Kim, *Eur. Polym. J.*, **44**, 3871 (2008).
5. B. Pang, C. Ryu, and H. Kim, *Mater. Sci. Eng. B*, **178**, 1212 (2013).
6. W. Yu, H. Xie, L. Yin, J. Zhao, L. Xia, and L. Chen, *Int. J. Therm. Sci.*, **91**, 76 (2015).
7. C. Leong and D. Chung, *Carbon*, **41**, 2459 (2003).
8. S. Shaikh, K. Lafdi, and E. Silverman, *Carbon*, **45**, 695 (2007).
9. J. Hong, J. Lee, C. Hong, and S. Shim, *Curr. Appl. Phys.*, **10**, 359 (2010).
10. L. C. Sim, S. R. Ramanan, H. Ismail, K. N. Seetharamu, and T. J. Goh, *Thermochim. Acta*, **430**, 155 (2005).
11. L. P. Zhang and Z. H. Xia, *J. Phys. Chem. C*, **115**, 11170 (2011).
12. M. Liu, X. B. Yin, E. U. Avila, B. S. Geng, T. Zentgraf, L. Ju, F. Wang, and X. Zhang, *Nature*, **474**, 64 (2011).
13. J. Pyun, *Angew. Chem. Int. Ed.*, **50**, 46 (2011).
14. Q. Wu, Y. X. Xu, Z. Y. Yao, A. R. Liu, and G. Q. Shi, *ACS Nano*, **4**, 1963 (2010).
15. C. Y. Lee, J. H. Bae, T. Y. Kim, S. H. Chang, and S. Kim, *Composites Part A*, **75**, 11 (2015).
16. S. Stankovich, R. D. Piner, S. T. Nguyen, and R. S. Ruoff, *Carbon*, **44**, 3342 (2006).
17. A. Pruna, D. Pullini, and D. Busquets, *J. Mater. Sci. & Tech.*, **31**, 458 (2015).
18. L. Z. Guan, Y. J. Wan, L. X. Gong, D. Yan, L. C. Tang, L. B. Wu, J. X. Jiang, and G. Q. Lai, *J. Mater. Chem. A*, **2**, 15058 (2014).
19. L. Cao, X. Liu, H. Na, Y. Wu, W. Zheng, and J. Zhu, *J. Mater. Chem. A*, **1**, 5081 (2013).
20. R. Qian, J. Yu, C. Wu, X. Zhai, and P. Jiang, *RSC Adv.*, **3**, 17373 (2013).
21. L. Huang, P. Zhu, G. Li, D. Lu, R. Sun, and C. Wong, *J. Mater. Chem. A*, **2**, 18246 (2014).
22. F. Du, W. Yang, F. Zhang, C. Y. Tang, S. Liu, L. Yin, and W. C. Law, *ACS Appl. Mater. Inter.*, **7**, 14397 (2015).
23. J. S. Shayed, A. Ehsani, M. R. Ganjali, P. Norouzi, and B. Jaleh, *Appl. Surf. Sci.*, **353**, 594 (2015).
24. Q. Huang, L. Zhou, X. Jiang, Y. Zhou, H. Fan, and W. Lang, *ACS Appl. Mater. Inter.*, **6**, 13502 (2014).
25. M. Al-Mamun, J. H. Lim, Y. E. Sung, and S. R. Kim, *Chem. Lett.*, **42**, 31 (2012).
26. T. Zhou, X.Wang, X. Liu, and D. Xiong, *Carbon*, **48**, 1171 (2010).
27. N. A. Kumar, H. J. Choi, Y. R. Shin, D. W. Chang, L. Dai, and J. B. Baek, *ACS Nano*, **6**, 1715 (2012).
28. J. Song, J. Qiao, S. Shuang, Y. Guo, and C. Dong, *J. Mater. Chem.*, **22**, 602 (2012).
29. S. Dutta, C. Ray, S. Sarkar, M. Pradhan, Y. Negishi, and T. Pal, *ACS Appl. Mater. Inter.*, **5**, 8724 (2015).
30. E. Makila, L. Bimbo, M. Kaasalainen, B. Herranz, A. Airaksinen, M. Heinonen, E. Kukk, J. Hirvonen, H. Santos, and J. Salonen, *Langmuir*, **28**, 14045 (2012).
31. F. Zhang, H. Jiang, X. Li, X. Wu, and H. Li, *ACS Catal.*, **4**, 394 (2014).
32. Q. Chen and N. L. Yakovlev, *Appl. Surf. Sci.*, **257**, 1395 (2010).
33. J. Yang, J. Li, X. Yang, X. Wang, L. Wan, and Y. Yang, *Mater. Chem. Phys.*, **135**, 687 (2012).
34. Z. Liu, H. Zhou, Z. Huang, W. Wang, F. Zeng, and Y. Kuang, *J. Mater. Chem. A*, **1**, 3454 (2013).
35. Y. Lin, J. Jin, and M. Song, *J. Mater. Chem.*, **21**, 3455 (2011).
36. G. H. Park, K. T. Kim, Y. T. Ahn, H. Lee, and H. M. Jeong, *J. Ind. Eng. Chem.*, **2014**, 4108 (2014).
37. Z. Czech, A. Kowalczyk, R. Pelech, R. J. Wróbel, L. Shao, Y. Bai, and J. Swiderska, *Int. J. Adhes. Adhes.*, **36**, 20 (2012).
38. J. K. Kim, J. W. Kim, M. I. Kim, and M. S. Song, *Macromol. Res.*, **14**, 517 (2006).